

Dimensional changes during binder removal in a mouldable ceramic system

K. E. HRDINA, J. W. HALLORAN

*University of Michigan, Department of Materials Science and Engineering,
Ann Arbor, MI 48109-2136, USA*

E-mail: john-halloran@mse.engin.umich.edu

Significant dimensional changes involving linear expansion and shrinkage of 6% occur during heating of a thermoplastic SiC/ethylene vinyl acetate (EVA) mixture. Thermal expansion occurs before weight loss begins, and can be quantitatively explained in terms of the thermal expansion behaviour of the constituents and the crystallization or melting of the semicrystalline polymer. Irreversible anisotropic displacements occur during the first heating cycle due to relaxation of moulding strains. These can be reduced by annealing for periods comparable to the viscoelastic relaxation of the ceramic/polymer system. Shrinkage occurs during the early stages of degradation of EVA. This shrinkage is quantitatively accounted for with volume losses resulting from removal of the EVA. Shrinkage continues as weight loss proceeds and stops only at the point the ceramic particles contact one another. Total displacement behaviour is the sum of the shrinkage from weight loss plus the expansion from thermal expansion of the individual components, and can be quantitatively predicted for simple or multi-step heating schedules. © 1998 Kluwer Academic Publishers

1. Introduction

Certain ceramic fabrication techniques, notably thermoplastic injection moulding, employ a substantial fraction of polymer binder. We report here observations of significant dilation and contraction of formed ceramics during heating through the binder removal stage. Although the dimensional tolerances of thermoplastically moulded ceramics are very important, dimensional changes in the early stages of binder removal have not been fully appreciated. Few researchers have focused on the dimensional changes that occur during binder removal and none have quantitatively described the whole displacement behaviour. It is inconvenient to observe dimensional changes during binder burnout, since the specimen is soft and the noxious effluents produced during binder removal tend to ruin delicate experimental instruments. A thermomechanical analyser (TMA) which was specifically designed for the binder removal process was built. This TMA applies a very small load to the sample so that dimensional changes can be measured in soft samples undergoing binder removal.

Anisotropic thermal expansion was observed in moulded cylinders by Zhang and Evans [1]. After annealing, the thermal expansion was isotropic, indicating the presence of residual stresses in the unannealed specimens which qualitatively explained the anisotropy. We report similar residual anisotropic strains in this paper. Edirisinghe and Evans [2] noted that the large dimensional changes occurring within crystalline polymers during cooling was associated with void or microcrack formation.

The thermal removal of ethylene co-vinyl acetate has been studied by Trunec and Cihlar [3] for EVA paraffinic wax binders with submicrometre alumina. They report that inert atmospheres are best for removing EVA. A vacuum promotes defect formation through boiling of low molecular weight constituents, while oxygen preferentially degrades the surface regions of the specimen and promotes non-uniform shrinkage. Inert atmospheres minimize the non-uniform shrinkage and thus produced defect-free parts. Earlier work by Wright *et al.* [4] noted that increases in packing density were observed in parts that underwent uniform degradation procedures, such as in inert atmospheres. It is for this reason that inert atmospheres were used in the present research.

Our observations are schematically illustrated in Fig. 1, a hypothetical displacement history during heating of a moulded ceramic specimen. Note that these displacements are large compared to a typical tolerance for finished ceramic parts (0.5–3.0%). Such dimensional changes, especially if anisotropic, could limit achievable tolerance. The initial expansion observed in Fig. 1 occurs as a result of the large thermal expansion of the polymer without much binder loss. Anisotropic expansion may occur at this stage due to residual strains remaining from moulding. The rate of binder removal increases at higher temperatures. Shrinkage occurs as the binder begins to degrade and the volume of material leaving the system is occurring at a faster rate than the volume increases from thermal expansion of the material. Once the temperature for densification is achieved, the part shrinks. Some small thermal shrinkage may

occur during cooling to room temperature from the sintering temperature.

2. Experimental procedures

2.1. Composition and processing

The thermoplastic ceramic system examined here is ethylene co-vinyl acetate* (a co-polymer commonly called ethylene vinyl acetate or EVA) blended with ceramic powders consisting of 90 wt % silicon carbide[†], 6 wt % aluminium oxide[‡] and 4 wt % yttrium oxide[§]. This SiC composition liquid phase sinters at 1880 °C [5, 6]. Certain samples also were blended with heavy mineral oil[¶], a paraffinic distillate. Some of the properties of the EVA polymer are presented in Table I.

The ceramic powders were mixed by ball milling in isopropanol for 24 h, using alumina grinding media, followed by drying. Blending of the powder with the resin was carried out in a heated shear mixer** with roller blades. The EVA resin was added first and melted under shear at 130 °C at a constant speed of 60 r.p.m. The ceramic powder was added in small increments of mixing for 1–2 min. The increased shear, upon adding the powder, increased mixing temperatures to 150–160 °C. The mineral oil, if used, was added next.

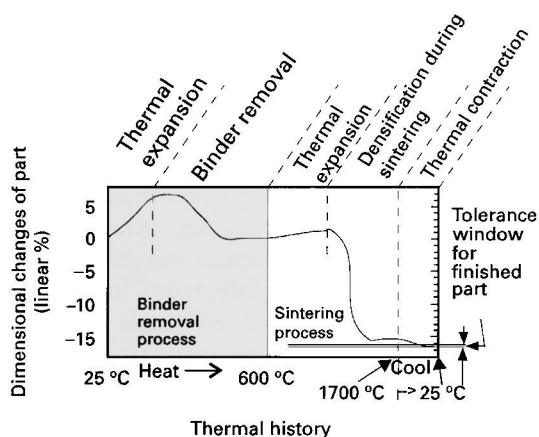


Figure 1 Hypothetical dimensional changes during processing of thermoplastically molded ceramic.

TABLE I Selected properties of the ethylene co-vinyl acetate polymer

Melt index: 0.7 dg min ⁻¹	$M_n = 100\,000$	$M_w = 250\,000$
$T_g = -20\text{ °C}$	$T_m = 84\text{ °C}$	Density = 0.941 g cm ⁻³
Per cent crystalline = 10%	Formula	Vinyl acetate (VA) content = 18 wt %
	$-\text{[(CH}_2\text{-CH}_2\text{)}_x\text{-(CH-CH}_2\text{)}_y\text{]}_n-$	
	$\begin{array}{c} \\ \text{O-C-CH}_3 \\ \\ \text{O} \end{array}$	

*ELVAX 470, Dupont.

[†] β -SiC, H.C. Starck grade B 10; SA = 14–17 m² g⁻¹, mps = 0.75 μ m.

[‡]Malakoff Industries, Inc., RC-HP DBM; SA = 7–8 m² g⁻¹, mps = 0.55 μ m.

[§]Johnson Matthey, mps = 1–2 μ m.

[¶]Heavy mineral oil, Mallinckrodt, paraffin-oil, sp. = 0.881.

**C.W. Brabender Instruments, Inc., PL 2000 Plasti-Corder with roller blade mixing heads.

††TGA-171, ATI-CAHN microbalance.

**Leco Corporation, Leco model 800-200.

The polymer-ceramic powder composition is reported as a nominal room temperature volume per cent, based on the room temperature densities of the components. The compositions are 51 vol % ceramic powder + 49 vol % co-polymer for the ceramic/EVA system, or 54.5 vol % ceramic + 39.5 vol % EVA + 6 vol % mineral oil for the systems containing mineral oil.

The actual weight per cent of binder in each material was determined by thermogravimetric analysis^{††} (TGA). Binder uniformity in a batched material and between batches of material was checked by the random selection of four specimens from two separate batches of material. These results indicate no significant differences between binder content within a batch of material or between batches. Disc-shaped specimens were fabricated by compression moulding in a 25.4 mm diameter uniaxial die^{¶¶} at 27 MPa and 125 °C. TGA analysis on moulded specimens showed that the binder distribution was uniform throughout the sample.

2.2. Displacement measurements

Dimensional changes were measured in a TMA designed specifically for studying the binder removal process of thermoplastic ceramics. Fig. 2 is a schematic of the instrument. The specimen rests on a platform at the bottom of an inner fused silica tube. A fused silica rod rests on top of a porous fused silica plate which in turn, rests on the specimen. The porous fused silica plate has 90–150 μ m pores to allow unimpeded binder removal while distributing the load that the rod places on the soft specimen. This plate reduces the pressure on the specimen during the test to about 1.4 kPa, so that deformation of the soft specimen is negligible. The LVDT core is attached to the push-rod, and the LVDT bore resides on a fused silica support above the furnace. Elaborate cooling means were used to thermally isolate the specimen from the LVDT core system to localize all dimensional changes to that of the specimen alone. A blank run from RT to 500 °C produced a displacement of only $\pm 1\text{ }\mu$ m.

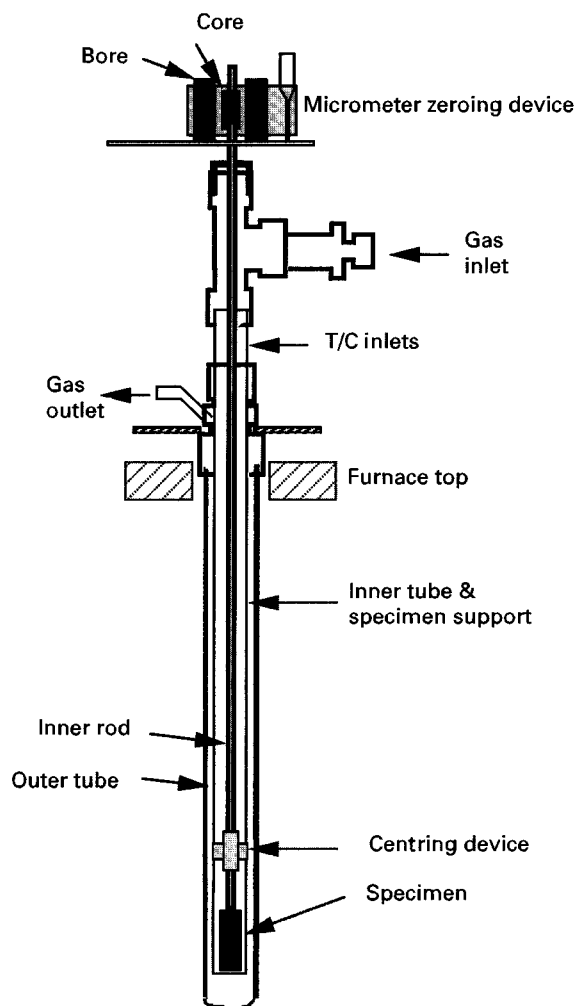


Figure 2 Thermomechanical analyzer (TMA) for controlled atmosphere binder removal study.

Nitrogen gas flows through the inner tube down to the specimen and then up through the annulus between the inner and outer tube to the exhaust port. The TMA is capable of operating from room temperature to temperatures over 800 °C in controlled atmospheres. The TMA was calibrated against a single crystal sapphire alumina specimen and was found to be accurate to 0.2 p.p.m. from room temperature to 500 °C.

Dimensional and weight loss measurements during binder removal were made on 3 mm thick moulded specimens. The specimens were sandwiched between a quartz disk on the bottom with a porous quartz disk placed on top of the specimens to both distribute the load and allow gas escape. The weight of the LVDT core and rod produced a nominal pressure of 1.4 kPa. Nitrogen was circulated past the specimen during heating. Weight loss measurements were made by the placement of duplicate specimens with duplicate quartz disks above and below the specimen in a TGA* heated at the same schedule as the TMA.

2.3. Rheological measurements

A cone and plate rheometer[†] was used for determination of relaxation times as a function of both

*TGA-171, ATI-CAHN microbalance.

†Bohlin CS-50 Rheometer.

TABLE II Composition of specimens examined in rheometer for relaxation times

Specimen	Ceramic (vol %)	EVA (vol %)	Mineral oil (vol %)
1	0	100	0
2	51	49	0
3	51	43	6
4	51	37	12
5	51	31	18

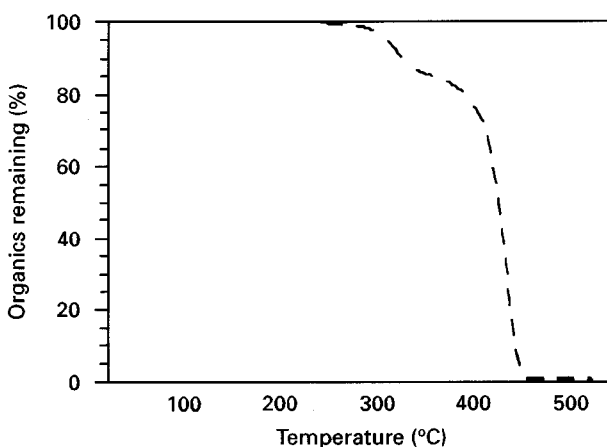


Figure 3 Thermogravimetric analysis (TGA) for unfilled ethylene vinyl acetate heated in nitrogen at 2 °C min⁻¹.

temperature and composition for the polymer and filled polymer. Specimens of the compositions listed in Table II were examined at temperatures of 110, 125, 135, 150 and 170 °C. These temperatures were above the melting point of the polymer (~ 85–100 °C) but below the temperatures at which appreciable degradation occurs (~ 190 °C). The tests were run at a constant stress level with strain measured.

3. Results and discussion

3.1. Removal of the EVA

As discussed in detail elsewhere [7, 8], EVA removal occurs in two distinct steps. As shown in Fig. 3, no weight loss occurs in nitrogen below 250 °C at a heating rate of 2 °C min⁻¹. Around 270 °C, the vinyl acetate elimination begins, which produces acetic acid. The acetic acid product is initially dissolved in the polymer, but diffuses to the surface where it is lost as gas. The solid residue of the EVA after acetate elimination is poly ethylene-co-polyacetylene. Acetic acid elimination is complete above 370 °C. Degradation of the poly ethylene-co-polyacetylene begins around 400 °C and is complete at 500 °C. The displacement behaviour is examined considering first the events which occur at relatively low temperatures before appreciable binder (~ 1%) has been removed. Later we will discuss events which occur at higher temperature, where significant amounts of binder are removed.

Fig. 4 shows the displacement observed for a moulded specimen of SiC in EVA and mineral oil

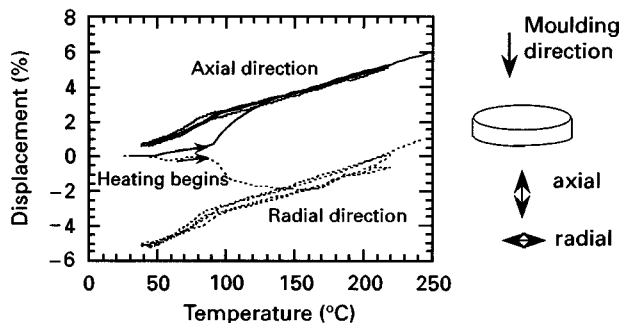


Figure 4 Displacement during thermal cycling between room temperature and 220 °C for compression molded discs of 54.5 vol. % SiC powder + 39.5 vol. % EVA + 6 vol. % mineral oil.

upon thermal cycling between RT and 220 °C, before EVA degradation begins. There is unique displacement behaviour taking place upon initial heating. The displacement is large (6 linear %) and anisotropic, with expansion occurring in the axial direction of the specimen and contraction occurring in the radial direction of the specimen. The anisotropic displacement only occurs during the first heating cycle. Upon subsequent cooling and heating, the specimen undergoes isotropic displacement. It should again be noted that both the reversible and irreversible displacement so far mentioned is occurring before any appreciable weight loss takes place. The reversible and irreversible displacements will be discussed separately.

3.2. Reversible displacement (before EVA removal begins)

The TMA data for one reversible thermal cycle is shown in Fig. 5 for a SiC filled sample with EVA and mineral oil. This section is concerned with the explanation of this phenomenon and its effect on binder removal. The expansion is quite large – about 4% – and there is a change in slope occurring at about 90 °C in the heating cycle and about 75 °C in the cooling cycle. This is the result of the melting and crystallization of the semicrystalline polymer. Differential scanning calorimetry (DSC) measurements were carried out to determine if the melting and crystallization temperatures of the EVA polymer correlated with the behaviour observed in the TMA. Fig. 6 shows both DSC and TMA data between 40 °C and 120 °C for another sample of SiC-filled EVA with mineral oil. This DSC behaviour is characteristic of polymeric melting and crystallization. The crystallization process is offset to lower temperatures from that of the melting process which is a result of the time dependent nucleation process for crystallization. It is evident that the melting and crystallization temperatures observed in the DSC correlate with the behaviour observed in the TMA.

The next task was to determine how well the measured thermal expansion behaviour of these filled polymers compared to those calculated assuming an ideal rule of mixtures for thermal expansion of a composite of ceramic powders in this polymer. For this, we use literature data for the thermal expansion of each phase

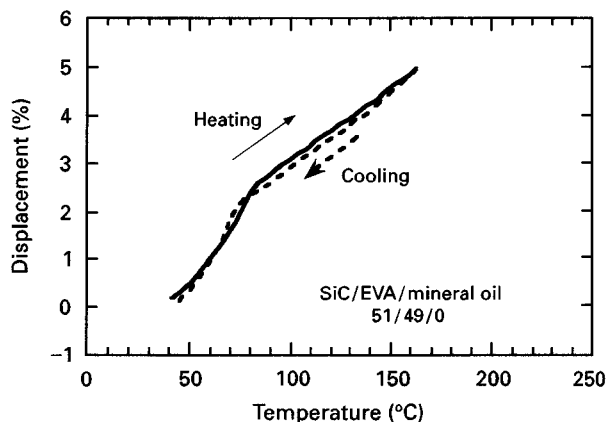


Figure 5 Reversible displacement occurring during thermal cycling in SiC/EVA specimen without mineral oil before appreciable weight loss.

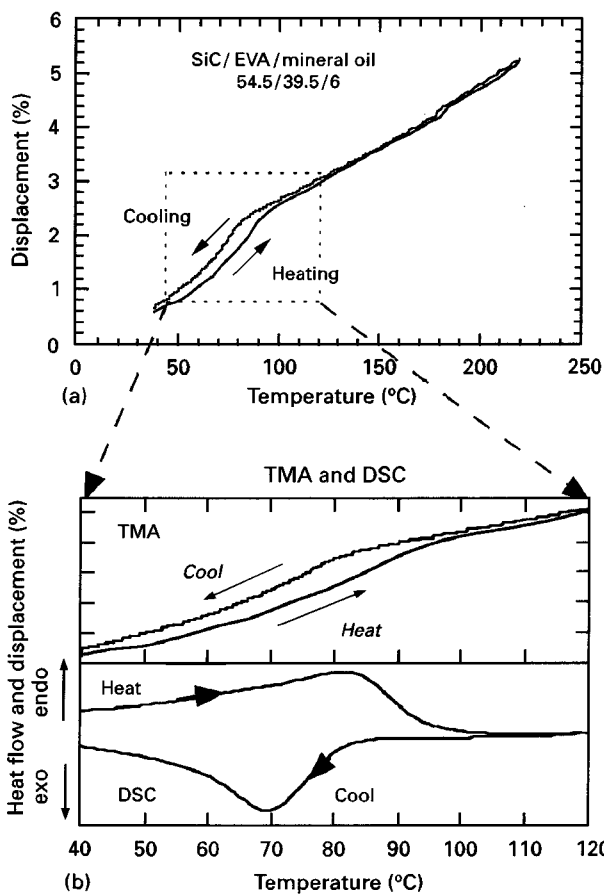


Figure 6 (a) Reversible displacement occurring during thermal cycling in a SiC/EVA/mineral oil specimen; (b) Enlargement of the TMA region between 40 °C and 120 °C and a DSC scan of the specimen in the same temperature range.

and their volume fractions. The fraction of the crystalline portion of the EVA co-polymer was from DSC experiments, using the enthalpy from the cooling cycle as a measure of the volume fraction crystalline EVA. Using a value of 287 J g⁻¹ for the enthalpy of fusion (ΔH_f) of crystalline polyethylene [9], we infer the fraction the EVA which is crystalline from the ratio of $\Delta H_{\text{measured}}$ and ΔH_f , a standard method [9]. The DSC results are summarized in Table III for four different types of samples. The third and fourth sample types

TABLE III Summary of DSC data

Type	Number of samples	Specimen composition (ceramic/EVA/ mineral oil) vol%	T_m (°C)	T_c (°C)	ΔH_f ($J g^{-1}$ of EVA)	% xtal.
I	3	0/100/0	90	74	29.9 ± 0.8	10.4 ± 0.3
II	3	0/75/25	88	72	29.4 ± 0.6	10.3 ± 0.2
III	3	54.5/39.5/6	85	71	17.9 ± 1.4	6.2 ± 0.5
IV	9	51/49/0	85	72	19.5 ± 0.4	6.8 ± 0.1

TABLE IV Volume fraction of phases

Phase	SiC/EVA/HMO 51/49/0	SiC/EVA/HMO 54.5/39.5/6
α -SiC	47.3	50.5
α -Al ₂ O ₃	2.5	2.7
Y ₂ O ₃	1.2	1.3
PE (amorphous EVA)	39.0	31.4
PVA (amorphous EVA)	6.7	5.4
Crystalline EVA	3.3	2.7
Mineral oil	None	6

were required for application of the ideal rule of mixtures while the other two sample types were run in order to study the effect of the addition of mineral oil and ceramic powder on crystallization in the EVA system.

The per cent crystallinity in the pure EVA copolymer (Type I) is about 10%. The addition of mineral oil resulted in a -2°C shift in the T_m and T_c temperatures, indicating some miscibility between mineral oil and EVA copolymer (Type II) [10, 11]. However, the mineral oil apparently did not affect the quantity of crystals formed in the copolymer blend. Within the fully loaded polymer systems (Types III and IV), the crystallinity is reduced from 10% in the neat copolymer to between 6.2 and 6.8% in the specimens containing 50 vol. % ceramic powder. Fillers are known to effect crystallinity in a polymer [9, 12]. The effect is dependent on both the quantity of filler as well as the interaction between the powder's surface and the polymer. Reduced crystallinity is an indication of "strong" interactions between the polymer and the ceramic which inhibits crystallization. The reduced melting point from 90°C for neat EVA to 85°C for the filled polymer indicates that the crystal growth rate has also been reduced in the presence of the filler [12].

The effective quantity of each phase is summarized in Table IV for the two filled systems whose thermal expansion behaviours were shown in Figs 5 and 6. EVA is a random copolymer composed of 82 wt % polyethylene and 18 wt % polyvinyl acetate. The thermal expansion values for EVA were obtained through application of the ideal rule of mixtures with thermal expansion data used from both polyvinyl acetate (PVA) and polyethylene (PE). The thermal expansion behaviour of petroleum distillates such as mineral oil depends on the specific gravity of the liquid [13, 14]. The thermal expansion of mineral oil was taken as the expansion value for a petroleum distillate with the same density (API density = 30 [15])[12].

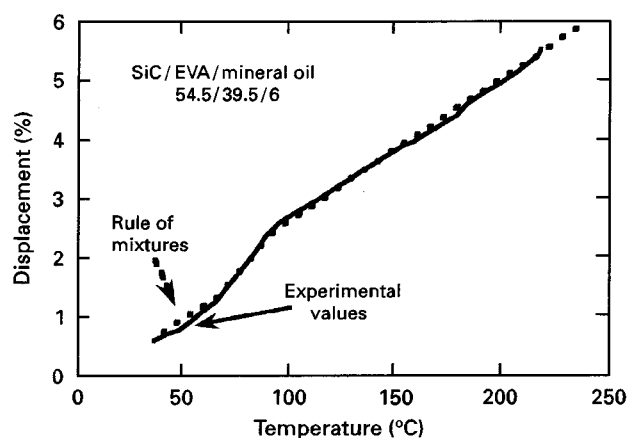


Figure 7 Comparison of experimental displacement (solid line) with calculations for thermal expansion using rule of mixtures (points).

Fig. 7 shows the results comparing the measured thermal expansion behaviour to the values calculated using the rule of mixtures for the specimens with mineral oil. An ideal rule of mixtures agrees well with the experimental behaviour of the specimen with mineral oil. Similar results were obtained for the specimen without mineral oil. Additional details are reported elsewhere [7]. The ideal rule of mixtures quantitatively describes the reversible displacement behaviour. It should be noted that the ideal rule of mixtures assumes that no strains either build up as a result of thermal expansion mismatch between the phases or are present prior to thermal expansion measurements. Residual strains were relieved, in this case, during the first thermal cycle.

3.3. Effect of temperature on the volume fraction of ceramic powder

The volume fraction of ceramic powder, ϕ , is usually considered to be a temperature-independent compositional variable, but in fact it has a significant temperature dependence. The reported value of 54.5 vol % solids loading is for room temperature only. As the batched material is heated, the polymer expands about 25 to 50 times more than does the ceramic phase. This leads to a decrease in the vol % of solids as the material is heated. Fig. 8 shows how the vol % solid loading changes during heating of a specimen within the lower temperature region before appreciable binder removal takes place. It is seen that increasing the temperature significantly lowers the filler level. The vol % solids loading drops by about 6% in this particular case, when heated from room temperature

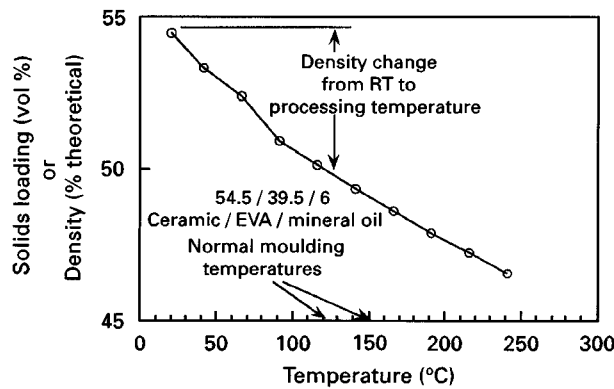


Figure 8 Decrease in volume fraction ceramic solids with temperature calculated from thermal expansion of the polymer for SiC/EVA/mineral oil.

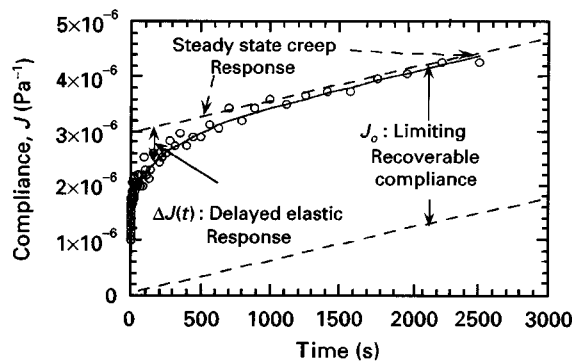


Figure 9 Compliance response of filled polymer at 125°C.

to the moulding temperature (125–150°C). The implications of this on rheological processes are discussed elsewhere [7].

3.4. Irreversible displacement (before EVA removal begins)

Recall from Fig. 4 that irreversible displacements were observed during the first heating cycle for the compression moulded discs, which featured extra axial expansion in the compression direction and contraction in the radial direction. The irreversible displacement involves viscoelastic relaxation phenomena. We digress at this point to discuss the viscoelastic behaviour of the ceramic-filled EVA.

The compliance response of the SiC/EVA, determined by cone and plate stress relaxation at 125°C is shown in Fig. 9. This shows the long term steady state creep at long times as well as the delayed elastic response or viscous response $\Delta J(t)$. Similar data were obtained at 110, 125, 135, 150, and 170°C, and used to determine the relaxation time versus temperature. A relaxation time, τ_{relax} , was obtained by assuming a simple exponential relationship in which

$$\Delta J(t) = J_o \exp(-t/\tau_{relax})$$

where t is time, $\Delta J(t)$ is the delayed viscous compliance, and J_o is the limiting recoverable compliance. This fit provides a remarkable representation of the data with a single relaxation time. The y -intercept of

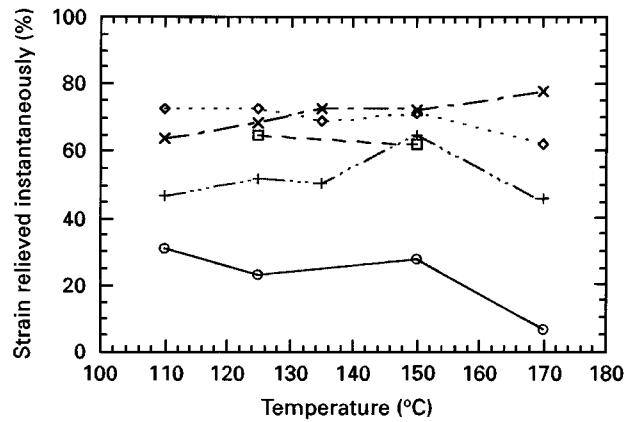


Figure 10 Instantaneous strain response vs. temperature for EVA, ceramic filled EVA with and without mineral oil. —○— neat EVA; mineral oil: —□— filled, 0%; —◇— filled, 6%; —×— filled, 12%; —+— filled, 18%.

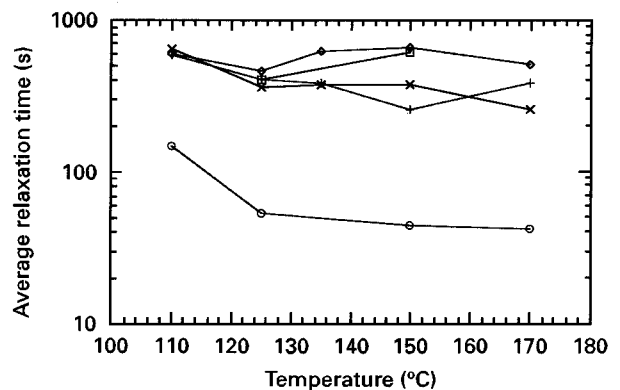


Figure 11 Viscoelastic relaxation time vs. temperature for EVA, ceramic filled EVA with and without mineral oil. —○— neat polymer; mineral oil: —□— filled, 0%; —◇— filled, 6%; —×— filled, 12%; —+— filled, 18%.

the plot also provides information about the instantaneous strain response of the system to an applied shear stress.

A fairly large instantaneous strain relief is coupled with the time dependent relaxation process in the current system. The instantaneous strain relief as a function of temperature and composition is plotted in Fig. 10. It is not surprising to see that the instantaneous amount of strain relieved is not appreciably affected by temperature or mineral oil content. This simply indicates that the elastic portion of the material is not significantly affected by either temperature or mineral oil content.

The filler increases the amount of relieved instantaneous strain from 20–30% for the unfilled polymer to 50–70% for the filled polymer. This is perhaps the result of increasing the volume fraction of material that behaves in a Hookian manner, i.e. the ceramic filler content. Larger instantaneous relieved strains are desirable since this minimizes the amount of possible residual strains remaining from specimen moulding.

The relaxation times as a function of temperature and mineral oil content are plotted in Fig. 11. The relaxation time is about 2.5 min at 110°C and 1 min at the moulding temperature of 125°C for the unfilled

polymer. The introduction of the ceramic powder increases this relaxation time to about 8 min. It is also evident from Fig. 11 that neither temperature nor mineral oil content drastically changed the relaxation time in the system which initially sounds counter-intuitive. Shorter relaxation times might be expected at higher temperatures or with increased mineral oil where increased polymer mobility occurs, but the data shows that this is not the case. This point deserves some comment. The relaxation time, τ , is related to the ratio of the composite viscosity, η_c , to the composite shear modulus, G_c :

$$\tau \propto \eta_c/G_c$$

The literature for filled polymers [16–18] indicates that the shear viscosity and shear modulus of the matrix phase and the filled composite system are related by:

$$\eta_c/\eta_m \approx G_c/G_m$$

where m and c denote the matrix phase and composite phases, respectively. This is true when the matrix phase is softer than that of the filler and when the Poisson's ratio is 0.5. The polymer is obviously softer than the ceramic material in the current system and the Poisson's ratio is typically 0.5 at temperatures above T_m for polymers [16–18] so that the above conditions for application of Equation 6 are likely to be fulfilled. Therefore, the trend in the relaxation time can be approximated by observing the trend in matrix behaviour from:

$$\tau \propto \eta_c/G_c \approx \eta_m/G_m$$

This indicates that the relaxation time depends on the mobility of the polymer and on its stiffness. The shear modulus and viscosity of the neat polymer was measured at various temperatures. The ratios of the polymer viscosity to shear modulus appear in Fig. 12 and show very little temperature dependence on relaxation time. This was indeed observed, as was shown in Figs 10 and 11. It is not surprising, in view of these results, that relaxation time is almost independent of temperature. A similar effect is therefore expected with changes in mineral oil content.

3.5. Correlating mould anneal time with irreversible displacement

The extent of irreversible expansion varied with moulding conditions such as time at pressure and cooling rate. Specimens were fabricated using the four different moulding conditions chosen to elucidate the origin and approximate magnitude of the anisotropic residual strains present in the moulded material. All samples were heated at 7°C min^{-1} to 125°C , where a pressure of 27 MPa was applied. Specimen 1 was held under pressure for only 1 min and rapidly cooled at $23^\circ\text{C min}^{-1}$. Specimen 2 held under pressure for 5 min, then rapidly cooled. Specimen 3 was held under pressure for 5 min, followed by a 10 min anneal at 125°C (no pressure), then rapidly cooled. Specimen 4 was the same as Specimen 3, but slowly cooled at $1.6^\circ\text{C min}^{-1}$.

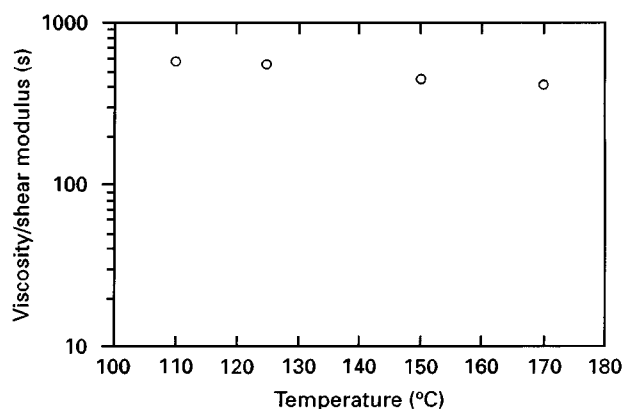


Figure 12 Ratio of viscosity to shear modulus vs. temperature for unfilled EVA.

Fig. 13a to d show the TMA results of these four tests. The unique axial expansion behaviour is seen during initial heating for each of the four different respective specimens. The magnitude of the irreversible displacement was largest for specimen 1 with a 2% irreversible linear expansion, compared to a 1% expansion for the other three specimens. There is little difference between the other three specimens (Fig. 13b to d), so cooling rate or increasing annealing time from 5 to 15 min has little effect. It appears that the filled polymer system has some memory of its previous shape that was not erased in the one minute during moulding, but an extra 5 to 15 min anneal cut the irreversible expansion in half. This corresponds to the 8 min relaxation time calculated from the cone and plate rheometer data.

The glass transition temperature (T_g) of the unfilled EVA polymer is -40°C . The irreversible displacement occurs when a moulded specimen is reheated to about 90°C , which is above the melting point of the polymer (Table III). This indicates that the crystallization process has inhibited polymer movement. The filler itself may also contribute, in part, to the immobilization process [12, 19]. DSC indicates significant interactions between the polymer and the ceramic as seen by the shift in T_m . Additionally, the quantity of filler and surface area of filler is quite large. Based on the surface area of the powder and volume fraction of filler, the average distance between powder particles is only 19.4 nm. This is on the order of the diameter of gyration of the EVA 470 which is calculated to be between 10 and 16 nm. It is likely that the ceramic filler contributes to the immobilization process in the polymer. The polymer crystallites, present as 6% of the polymer phase also exists in the small 19.4 nm spacing between particles. It is not surprising to see immobilized polymers at temperatures below the T_m of the polymer.

3.6. Displacement during binder removal

The displacement behaviour from room temperature to 500°C is shown in Fig. 14a, as a plot of displacement and temperature versus time for the complete binder removal process. This sample had a simple heating profile with two ramp rates. After thermally expanding by almost 6% after 20 h, the specimen

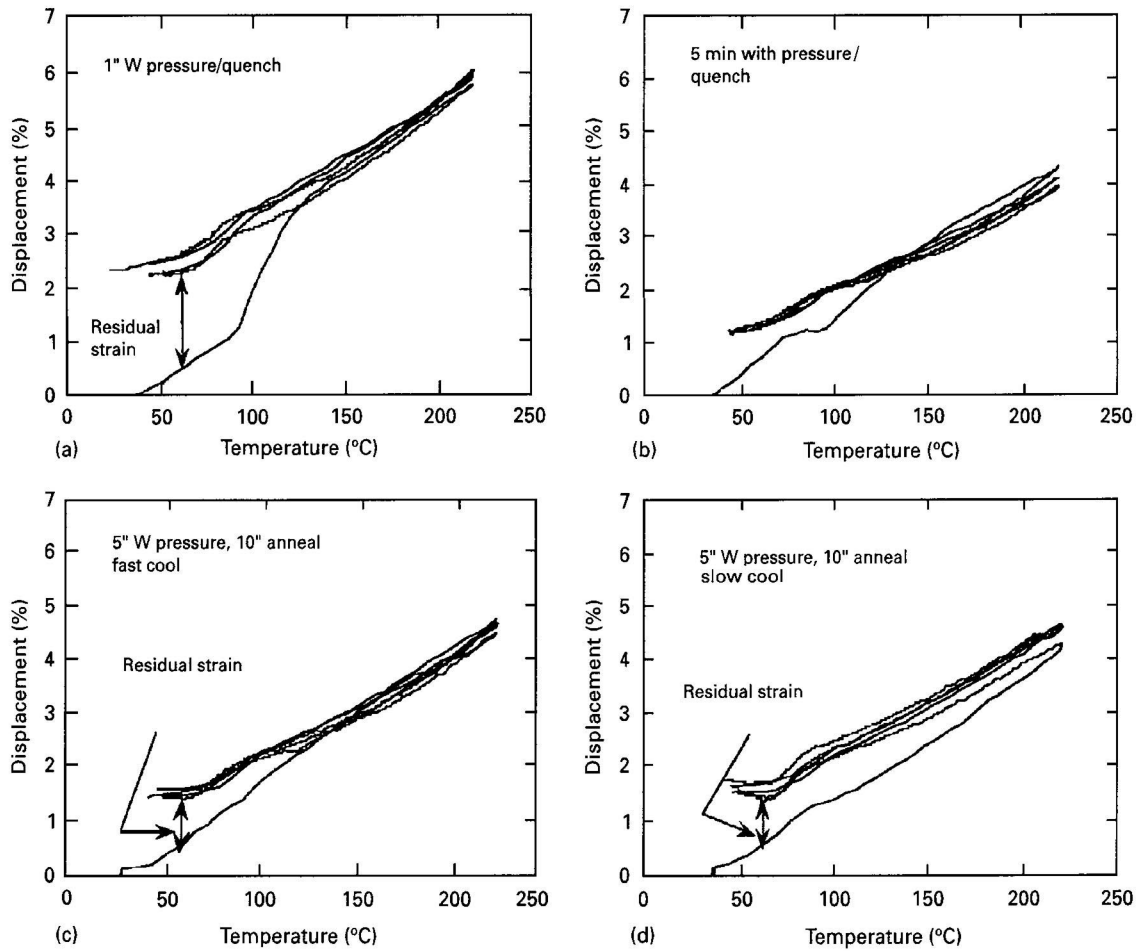


Figure 13 Effect of molding conditions on irreversible displacement in filled specimens.

begins to shrink. The shrinkage continues for another 20 h, then stops for the remaining 8 h of heating. The net dimensional change of the sample is only -0.5% , compared to the original as-moulded dimension. However, the shrinkage is -7.0% with respect to the point of maximum expansion.

Fig. 14b displays the same data as displacement versus temperature for the same 2-ramp heating process. Note that most of the shrinkage occurs in two narrow temperature ranges around 300°C and 380°C . Also shown in Fig. 14b is the weight loss data for a similar TGA sample with the same 2-ramp process. Most of the expansion occurs before weight loss begins. The 300°C shrinkage coincides with first stage weight loss and the 380°C shrinkage coincides with second stage weight loss behaviour. Note also the small displacement that occurs at 38 h in Fig. 14a. This was observed in many samples. It may be associated with intrusion of porosity into the sample, which causes similar displacements during drying [20].

The displacement and weight loss data are combined in Fig. 15 showing displacement versus the

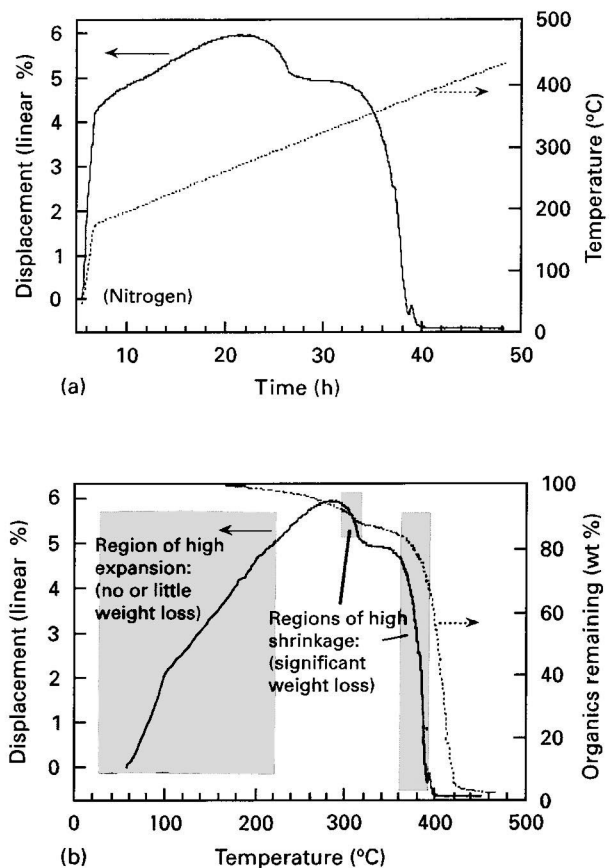


Figure 14 (a) Displacement behaviour vs. time and temperature vs. time during entire binder removal process; (b) displacement behaviour vs. temperature and remaining organics vs. temperature during entire binder removal process.

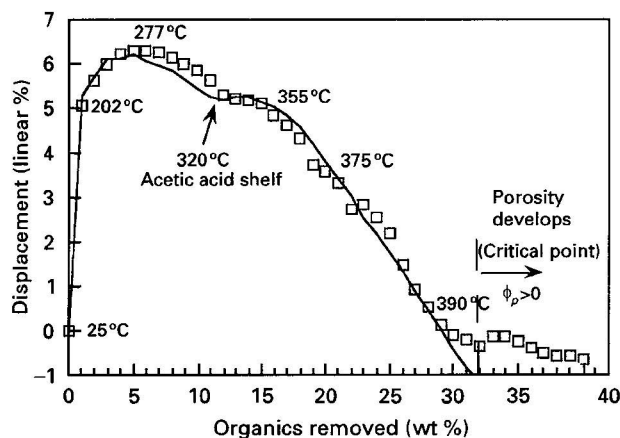


Figure 15 Displacement behaviour during binder removal as displacement vs. organic removal, showing experimental data and theoretical calculations, $2^{\circ}\text{C min}^{-1}$ to 170°C ; $0.1^{\circ}\text{C min}^{-1}$ to 500°C nitrogen (—) Theoretical; (\square) Experimental.

fraction of organics which have been removed. Each experimental point represents a different temperature, which is shown for a few points. After the initial thermal expansion, the sample shrinks as polymer is removed. Shrinkage continues until about 30% of the organics have been removed. We assume this point is analogous to the critical point in drying [21]. No porosity forms before the critical point. Porosity develops beyond the critical point.

The entire displacement behaviour of filled polymers within the initial stage of binder removal is actually the result of two competing phenomena. First, the specimen expands as a result of thermal expansion with increasing temperature and additional expansion as a result of the semicrystalline polymer melting. The second competing phenomena is the shrinkage resulting from evaporation of the evolving species. The total observed displacement is the sum of the expansion and shrinkage. During initial heating to about 250°C , there is little weight loss, so expansion occurs. At higher temperatures, the binder is removed with very little increase in temperature and shrinkage dominates. Shrinkage continues until the ceramic particles directly contact other ceramic particles. At this point, further shrinkage is prevented.

Also shown in Fig. 15 are theoretical calculations of displacement calculated with the assumption that displacement is a sum of the two terms mentioned above. The first term, the thermal expansion, was calculated using the ideal rule of mixtures as described previously. The second term, the volume shrinkage, needed to take into account the volume of material removed at the temperature at which the material was removed. This was calculated from the weight loss and density at temperature. The details are reported elsewhere [7]. The theoretical calculations involved no adjustable parameters, and were based on the following assumptions: (1) The thermal expansion behaviour of amorphous PVA and PE could be extrapolated through all temperatures used. (2) No porosity develops. (3) Weight loss behaviour in TMA was the same as in the TGA, indicating no temperature difference between specimens. These assumptions appear to be

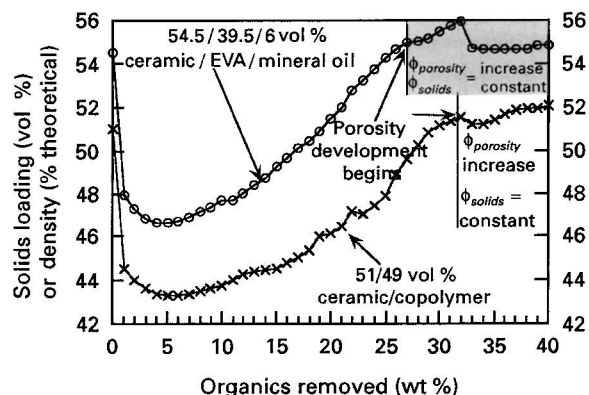


Figure 16 Calculated volume fraction ceramic solids vs. organics removed.

valid since the two curves match quite well, as seen in Fig. 15. Therefore, displacement behaviour of the entire binder removal process is quantitatively described.

As previously noted, the polymer phase expands much more than the ceramic phase during heating. This has led to a decrease in the vol % of solids as the material is heated. Fig. 16 shows the change in vol % solids loading during the entire binder removal process for a specimen with 51% ceramic + 49% EVA and another with 54.5% ceramic + 39.5% EVA + 6% mineral oil (all compositions as room temperature vol %). The initial drop in solids loading is a result of the polymer preferentially thermally expanding more than the ceramic phase. The solids loading again increases as polymer removal proceeds and polymer is removed. Note that the ceramic content drops (in the second case) from 54.5% to 47%, then increases to about 55%, a traverse of 7.7 vol % with relatively little net change after the binder is gone. Such dimensional changes would usually go unnoticed. At the minimum of ceramic volume fraction, the green ceramic should be quite soft. While we have no data on the actual mechanical properties of the ceramics during burnout, we can speculate that the temperature range of minimum ceramic volume fraction is where the risk of slumping is severe.

3.7. Effect of heating schedule on displacement history

Typically in ceramic practice, the binder removal schedule is a sequence of ramps instead of the simple 2-ramp schedule discussed previously. A typical multi-step series of eight ramps and seven isothermal holds is shown in Fig. 17 with the resultant displacement and weight loss behaviour during the entire binder removal process. Fig. 17a displays displacement versus time, and Fig. 17b shows displacement versus temperature. The peaks in the displacement versus time occur due to thermal expansion during ramps. The sharp drops in displacement versus temperature reflect shrinkage as material is removed during isothermal holds. Isothermal holds result in weight loss with no temperature change. The theoretically predicted and experimentally observed displacement

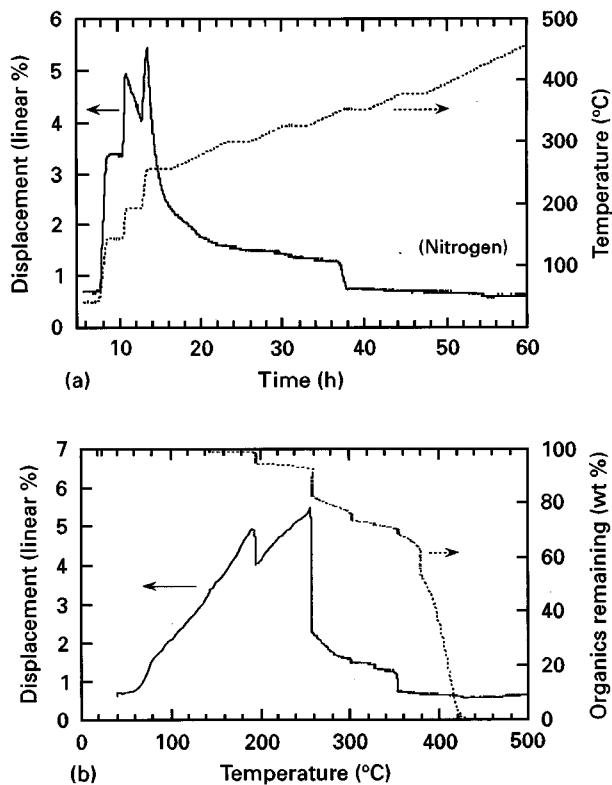


Figure 17 (a) Multiple-step heating schedule and resultant displacement behaviour vs. time during entire binder removal process; (b) displacement and weight loss behaviour vs. temperature.

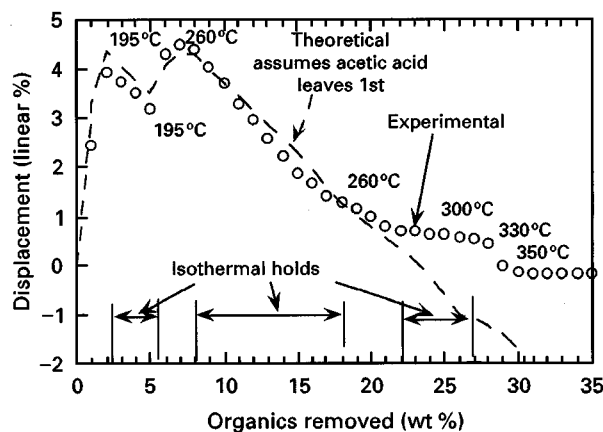


Figure 18 Displacement behaviour during binder removal with multiple-step schedule comparing experimental with calculated behaviour.

behaviour for this heating schedule is shown in Fig. 18. The theory agrees well with the observed displacements for the 195°C isotherm and the 260°C isotherm, but deviates from the observed shrinkage at the 300°C isotherm. It is common practice in ceramics to design binder removal schedules from TGA weight loss data, choosing slow heating at points of rapid weight loss to avoid defects. It is clear from the TMA displacement data that the ceramic bodies are also actively expanding and contracting, and this may be important in common mechanical defects such as warping and cracking.

Fig. 19 illustrates how the heating schedule can change the displacement history and final density after

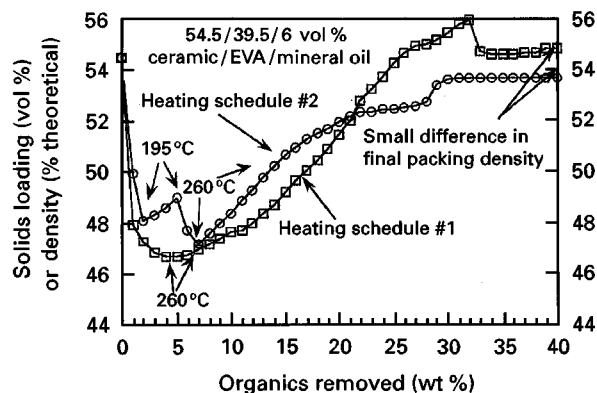


Figure 19 Density changes computed from displacement for two heating schedules.

binder removal. It compares a plot of ceramic volume fraction versus per cent organics removed for two heating schedule. Schedule #1 is a simple schedule with heating at 120°C h⁻¹ to 260°C, hold 2 h, heat 6°C h⁻¹ to 450°C. Schedule #2 is the multi-step schedule illustrated in Fig. 17. These two schedules create different paths of density versus organic content. The multi-step schedule avoids the minimum in ceramic density in the early stage of removal, but has a slightly lower density after the dimensional changes stop. The density of both specimens after the binder has been removed is essentially the same as the starting density.

Normal binder removal schedules use fast heating rates during cooling from the mould and fast heating rates up to the temperature at which binder removal starts. This minimizes process time. However, the results in this research suggest that minimum time may be obtained at the expense of part quality. Three suggestions are made with regards to thermal control during processing for improved quality. First, the part may require annealing in the mould to erase previous system "memory". Secondly, the part should be slowly cooled through the polymer crystallization process in order to minimize frozen-in residual strains from anisotropic cooling. Thirdly, the part should be heated slowly past the polymer melting process to minimize thermal gradients and warping from anisotropic heating effects.

4. Conclusions

Significant dimensional changes, representing 6 linear % expansion and shrinkage, occur during heating of the ceramic/EVA system. Expansion occurs at low temperatures before weight loss begins, and can be quantitatively explained in terms of the thermal expansion behaviour of the constituents and the crystallization or melting of the semicrystalline polymer. Irreversible anisotropic displacements occur during the first heating cycle due to relaxation of moulding strains. The irreversible displacements can be reduced by annealing at 125°C for times comparable to the viscoelastic relaxation time, which was determined to be 8 min for this ceramic/EVA system. Temperature and mineral oil content did not significantly effect this relaxation time.

Significant shrinkage occurs during the early stages of the degradation of EVA. This shrinkage is quantitatively accounted for with volume losses resulting from removal of the EVA. Shrinkage continues as weight loss proceeds and stops only at the point the ceramic particles contact one another. Further weight loss results in pore development. Total displacement behaviour is the sum of the shrinkage from weight loss plus the expansion from thermal expansion of the individual components, and can be quantitatively predicted for simple or multi-step heating schedules.

Due to thermal expansion of the polymer, the volume fraction of ceramic powder was shown to change significantly during the heating of the specimen.

Acknowledgement

This research was supported by the Defense Advanced Research Projects Agency and the Office of Naval Research through grant N00014-94-1-0278.

References

1. T ZHANG and J. R. G. EVANS, *J. Mater. Sci. Lett.* **9** (1990) 672.
2. M. J. EDIRISINGHE and J. R. G. EVANS, *J. Mater. Sci.* **22** (1987) 2267.
3. M. TRUNEC and J. CIHLAR, *J. Eur. Ceram. Soc.* **17** (1997) 203.
4. J. K. WRIGHT, M. J. EDIRISINGHE, J. G. ZHANG and J. R. G. EVANS, *J. Am. Ceram. Soc.* **73** (1990) 2653.
5. M. A. MULLA and V. D. KRSTIC, *J. Mater. Sci.* **29** (1994) 934.
6. DO-HYEONG KIM and CHONG HEE KIM, *J. Am. Ceram. Soc.* **73** (1990) 1431.
7. K. E. HRDINA in "Phenomena During Thermal Removal of Binders", PhD thesis, University of Michigan, (1997) p. 186.
8. K. E. HRDINA, J. W. HALLORAN, M. KAVIANY, and A. M. OLIVEIRA, *J. Mater. Sci.* in press.
9. U. S. RAMELOW and N. GUIDRY, *Microchem. J.* **50** (1994) 57.
10. N. E. CLOUGH, R. W. RICHARDS and T. IBRAHIM, *Polymer* **35** (1994) 1044.
11. O. OLABISI, L. M. ROBESON and M. T. SHAW, in "Polymer-Polymer Miscibility", (Academic Press, NY, 1979) p. 182.
12. Y. S. LIPATOV, in "Physical Chemistry of Filled Polymers", (International Polymer Science and Technology Monograph No. 2, translated from Russian by R. J. Moseley, 1979) p. 41.
13. R. H. PERRY, D. W. GREEN, and J. O. MALONEY, in "Perry's Chemical Engineering Handbook", 6th Edn, (McGraw-Hill, NY, 1984) p. 9.
14. W. F. BLAND and R. L. DAVIDSON, in "Petroleum Processing Handbook", (McGraw-Hill Book Company, NY, 1967) p. 12.
15. Penrico Product Bulletin for Drakeol 35 Heavy Mineral Oil.
16. L. E. NIELSEN, and R. F. LANDEL, in "Mechanical Properties of Polymers and Composites", 2nd Edn, (Marcel Dekker, NY, 1994) pp. 109, 384 and 64.
17. N. J. MILLS, *J. Appl. Polym. Sci.* **15** (1971) 2791.
18. N. S. ENIKOLOPYAN, M. L. FRIDMAN, I. O. STALNOVA and V. L. POPOV, in "Filled Polymers I Science and Technology", N. S. Enikolopyan, (Springer-Verlag, NY, 1990) p. 1.
19. J. L. KOENIG, and C.-H. CHIANG, The Role of the Polymeric Matrix in the Processing and Structural Properties of composite Materials, edited by J. Seferis, and L. Nicolais, (Plenum Press, New York, 1983) p. 503.
20. G. W. SCHERER, *Ceram. Trans.* **12**, in "Ceramic Powder Science III", edited by G. L. Messing and H. H. Technische (Am. Ceram. Soc., Inc., Ohio, 1990) p. 561.
21. G. W. SCHERER, *J. Am. Ceram. Soc.* **73** (1990) 3.

Received 30 July 1997

and accepted 13 February 1998